Vol. 2 • No. 5 • May • 2012

www.advenergymat.de

ADVANCED ENERGY MATERIALS

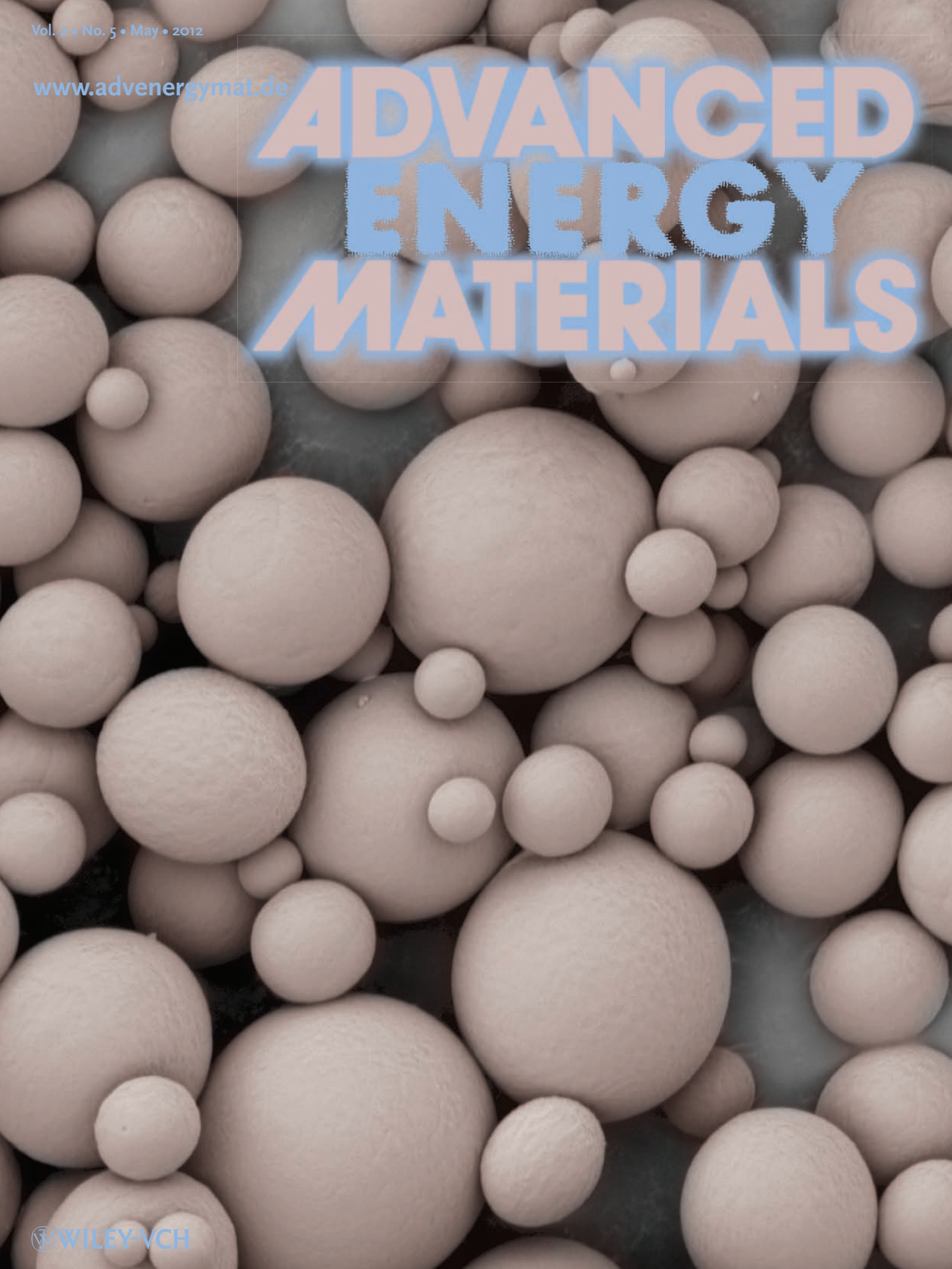

WILEY-VCH

Autonomic Shutdown of Lithium-Ion Batteries Using Thermoresponsive Microspheres

*Marta Baginska, Benjamin J. Blaiszik, Ryan J. Merriman, Nancy R. Sottos, Jeffrey S. Moore, and Scott R. White**

Autonomic, thermally-induced shutdown of Lithium-ion (Li-ion) batteries is demonstrated by incorporating thermoresponsive polymer microspheres (ca. 4 μm) onto battery anodes or separators. When the internal battery environment reaches a critical temperature, the microspheres melt and coat the anode/separator with a nonconductive barrier, halting Li-ion transport and shutting down the cell permanently. Three functionalization schemes are shown to perform cell shutdown: 1) poly(ethylene) (PE) microspheres coated on the anode, 2) paraffin wax microspheres coated on the anode, and 3) PE microspheres coated on the separator. Charge and discharge capacity is measured for Li-ion coin cells containing microsphere-coated anodes or separators as a function of capsule coverage. For PE coated on the anode, the initial capacity of the battery is unaffected by the presence of the PE microspheres up to a coverage of 12 mg cm^{-2} (when cycled at 1C), and full shutdown (>98% loss of initial capacity) is achieved in cells containing greater than 3.5 mg cm^{-2}. For paraffin microspheres coated on the anode and PE microspheres coated on the separator, shutdown is achieved in cells containing coverages greater than 2.9 and 13.7 mg cm^{-2}, respectively. Scanning electron microscopy images of electrode surfaces from cells that have undergone autonomic shutdown provides evidence of melting, wetting, and resolidification of PE into the anode and polymer film formation at the anode/separator interface.

1. Introduction

Li-ion batteries are vital energy storage devices due to their high specific energy density, lack of memory effect, and long cycle life.[1–4] They are predominantly used in consumer electronics; however, improvements in safety are required for full acceptance of Li-ion cells in transportation applications, such as electric vehicles or aerospace systems.[5,6] The presence of a volatile, combustible electrolyte and an oxidizing agent (lithium oxide cathodes) makes the Li-ion cell susceptible to fires and explosions.[7] According to the Federal Aviation Administration (FAA), from 1991 to 2010, there were 113 battery-related air incidents involving fire, smoke, extreme heat, or explosion.[8] Thermal overheating, electrical overcharging, or mechanical damage can trigger thermal runaway and when left unchecked, combustion of battery materials.

When a Li-ion battery cell exceeds a critical temperature (ca. 150 °C), exothermic chemical reactions are initiated between the electrodes and the electrolyte, raising the cell's internal pressure and temperature.[9–13] The increased temperature accelerates these chemical reactions, producing more heat through a dangerous positive feedback mechanism that leads to thermal runaway.[5,14] Further, the onset temperature of thermal runaway in Li-ion batteries decreases with increasing state of charge, making Li-ion cells even more susceptible to explosive failure.[15,16]

To prevent catastrophic thermal failure in commercial Li-ion batteries, either positive temperature coefficient (PTC) elements or shutdown separators are used. PTC elements exhibit a large increase in resistance upon thermal activation, halting the flow of current at the battery terminal.[14] Shutdown separators rely on a phase change mechanism to limit ionic transport via formation of an ion-impermeable layer between the electrodes.[17,18]

Shutdown separators typically consist of a poly(ethylene)-(PE)–polypropylene(PP) bilayer or a PP–PE–PP trilayer structure. Above a critical temperature, the porous PE layer softens, collapsing the film pores and preventing ionic conduction, while the PP layer provides mechanical support. However, when the internal cell temperature rises to the softening temperature of

M. Baginska, R. J. Merriman, Prof. S. R. White
306 Talbot Laboratory
Department of Aerospace Engineering
University of Illinois Urbana-Champaign
104 S. Wright Street, Urbana, IL, 61801, USA
E-mail: swhite@illinois.edu
Dr. B. J. Blaiszik, Prof. N. R. Sottos
Department of Materials Science and Engineering
Materials Science and Engineering Building
University of Illinois Urbana-Champaign
1304 W. Green St., Urbana, IL, 61801, USA
Prof. J. S. Moore
Department of Chemistry
University of Illinois Urbana-Champaign
505 South Mathews Avenue, Urbana, IL, 61801, USA
M. Baginska, Dr. B. J. Blaiszik, Prof. N. R. Sottos,
Prof. J. S. Moore, Prof. S. R. White
Beckman Institute for Advanced Science and Technology
University of Illinois Urbana-Champaign
405 N. Mathews Ave, Urbana, IL 61801, USA

DOI: 10.1002/aenm.201100683

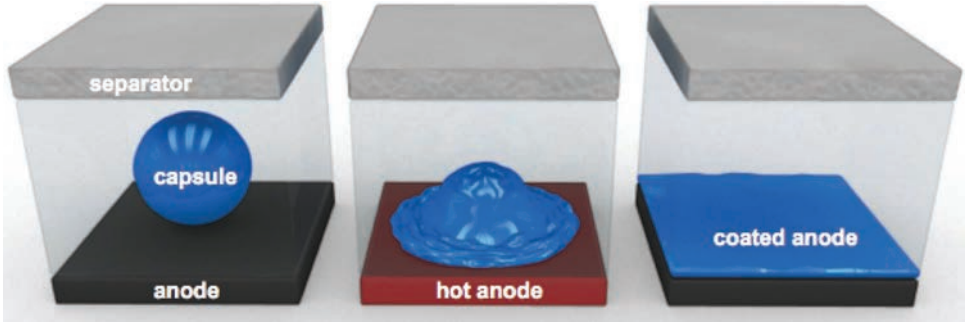

Figure 1. Schematic representation of microsphere-based shutdown concept for Li-ion batteries. Electrodes are functionalized with thermoresponsive microspheres which, above a critical internal battery temperature, undergo a thermal transition (melt). The molten capsules coat the electrode surface, forming an ionically insulating barrier and shutting down the battery cell.

the separator, the separator shrinks because of residual stresses induced during stretching of the separator films and the difference in density between the crystalline and amorphous phases of the separator materials.[19] In a PP–PE–PP trilayer structure, there is a buffer of only 35 °C between the melting point of PE (130 °C) and the melting point of PP (165 °C). If cell temperature continues to increase post-shutdown as a result of thermal inertia, the separator can fail, exposing the electrodes to internal shorting.[14,20] In some cases, cells with a shutdown separator remain shutdown for as little as 3 min before failing due to internal shorting.[21]

Other shutdown separators for Li-ion batteries have been reported in patent literature. Faust et al. described placing a wax-coated fabric between an electrode and the separator, where the wax on the fabric melts to close separator pores,[22] and Ullrich et al. described a sintered wax particle-coated electrode for thermal shutdown.[23] Electrolyte additives[12,14,24–27] thermally stable electrode materials,[28–32] and electrolytes capable of thermally triggered cross-linking[33] are also being investigated as thermal protection mechanisms to improve battery safety.

Our approach to improving the safety of Li-ion batteries is through the incorporation of functional microspheres into battery components. Microspheres can be engineered to respond to a variety of stimuli, including pressure,[34–38] pH,[39–41] electric fields,[42–45] magnetic fields,[46–49] and temperature.[50–53] Due to the inherent role of temperature in reactions occurring between electrolytes and electrodes near thermal runaway conditions, we propose the use of thermoresponsive microspheres to perform autonomic shutdown (**Figure 1**). In this concept, battery electrodes or the separator are coated with polymer microspheres (PE or paraffin wax) that undergo a thermal transition (melt) at a predetermined trigger temperature. The molten material is envisioned to wet the interface and provide an ion-insulating barrier, which prevents further battery operation.

The proposed microsphere-based shutdown mechanism offers significant advantages over current shutdown separator technology. First, unlike commercial shutdown separators which shrink and risk electrode shorting, ionic conduction is blocked by in situ formation of a conformal polymer film on the electrode surface. Second, PE microsphere technology can be used in conjunction with trilayer separators for an increased level of battery safety. Third, a wide range of polymer microspheres can be used in order to optimize shutdown response by tailoring trigger temperature, rate of shutdown, and thermomechanical stability for specific battery designs. Finally, a capsule-based approach provides the opportunity for multifunctional response beyond thermal shutdown, including the delivery of protective or restorative chemical species.

2. Results

2.1. Microsphere Preparation and Characterization

PE microspheres were prepared using a solvent evaporation technique. PE (8 g) was dissolved in xylenes (55 mL) at 75 °C. The PE-xylene mixture was added to 150 mL of an aqueous surfactant mixture consisting of 1 wt% Brij 76 (75 mL) and 1 wt% sodium dodecyl sulfate (SDS; 75 mL). The combined mixture was heated to 90 °C and mechanically stirred at 1000 rpm. The xylene was allowed to evaporate for 30 min under continuous agitation, at which point an additional 90 mL of the Brij/SDS surfactant mixture was added to the reaction beaker. Stirring was continued for an additional 30 min, at which point the reaction beaker was removed from the heated bath. Microspheres were gravimetrically separated from the reaction solution, decanted, centrifuged and rinsed three times with deionized water to remove excess surfactant. PE microspheres prepared with this method have a smooth exterior surface (**Figure 2**, inset) and are polydisperse in diameter. A histogram of capsule diameter (Figure 2) shows a bimodal distribution with a number average and weight average diameter of 4 μm and 9 μm, respectively. The melting point of PE microspheres was determined to be 105 °C by DSC analysis (Supporting Information (SI), Figure S1).

Paraffin wax microspheres were prepared using a meltable dispersion technique. Paraffin wax (20 g) was melted at 65 °C and added to 175 mL of an aqueous surfactant mixture of 1% poly(vinyl alcohol) (25 mL) and deionized water (150 mL). The combined mixture was heated to 70 °C and mechanically stirred at 2000 rpm. After emulsifying for 2 min, deionized ice-water (500 mL at 0 °C) was added to the reaction beaker to solidify the paraffin microspheres. Microspheres were rinsed to remove excess surfactant and air-dried. The resulting capsules have a rough surface morphology (SI, Figure S2) and have a number

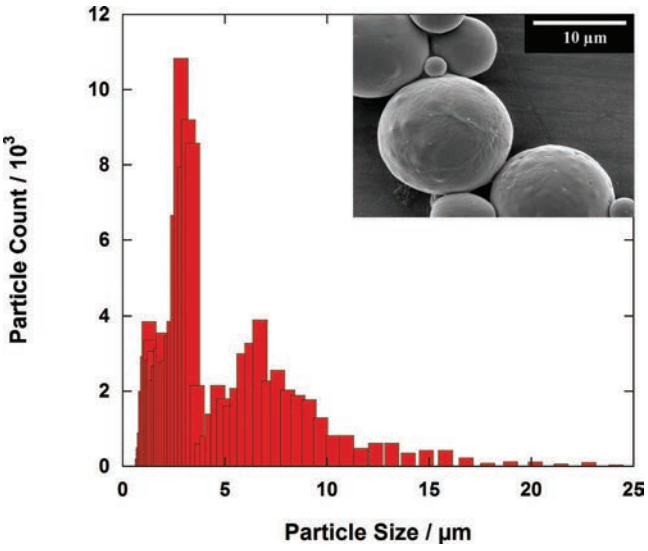

Figure 2. Histogram of PE capsule diameter. Inset: scanning electron microscopy (SEM) image of PE microsphere surface morphology.

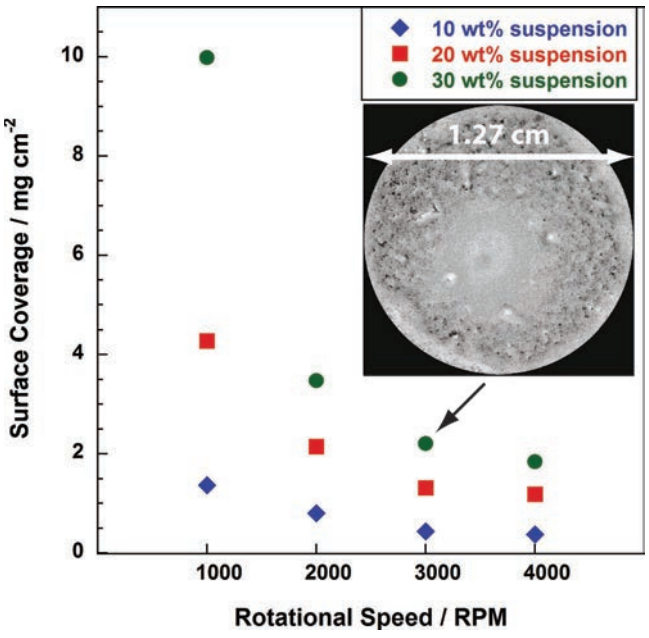

Figure 3. Characterization of anodes coated with thermally-triggered PE microspheres. Inset: optical image of a representative anode surface after spin-coating at 3000 rpm from a 30 wt% suspension of PE microspheres in NMP solvent.

average diameter of 42 μm and a weight average diameter of 47 μm.

2.2. Electrode and Separator Functionalization

PE and paraffin wax microsphere coated anodes were prepared by spin-coating a suspension of microspheres onto graphitic anode disks (1.27 cm dia.). The microsphere suspension was prepared by combining microspheres with poly(vinylidene fluoride) binder in a 10:1 ratio, and mixing with varying amounts of n-methyl pyrrolidone (NMP) solvent. The suspension was then manually stirred to ensure a homogeneous dispersion of binder. We define the surface coverage (ρ) of microspheres on a substrate material as $\rho = m_{capsule}/SA_{substrate}$, where $m_{capsule}$ is the mass of capsules functionalized onto the substrate and $SA_{substrate}$ is the surface area of the substrate. The surface coverage of microspheres on each anode was controlled by adjusting the concentration of microspheres in the suspension and the rotation speed of the spin-coater (**Figure 3**). Higher surface coverage was obtained by increasing the concentration of microspheres in suspension or by reducing the rotation speed. A representative anode surface after spin-coating at 3000 rpm from a 30 wt% suspension of PE microspheres in NMP solvent is shown in Figure 3, inset. During the spinning process microspheres tend to accumulate near the edge of the anode and during the drying process some aggregation of microspheres is evident. Profilometry of an anode with ρ = 5.5 mg cm^{-2} gives an RMS roughness of 5.9 micrometers, compared to an RMS roughness of 1.5 micrometers for a control anode (ρ = 0 mg cm^{-2}).

A similar procedure was used to functionalize commercial trilayer PP–PE–PP Celgard 2325 separators (1.75 cm dia.) with PE microspheres. Surface coverage characterization for the coated separators is presented in SI, Figure S3. Higher surface coverage separators can be obtained by depositing the microsphere suspension onto the separator without spin-coating and allowing the separator to air dry.

Following electrode functionalization, anodes and separators were assembled into coin cells containing $Li(Ni_{1/3}Co_{1/3}Mn_{1/3})O_2$ cathodes and 1.2 M $LiPF_6$ in ethylene carbonate (EC):ethyl methyl carbonate (EMC) solvent in a 3:7 ratio.

2.3. Coin Cell Testing

The shutdown performance of coin cells containing coated anodes (or separator) was assessed using CR2032 type Li-ion coin cells. Cells were first cycled at the 1C rate from 3 to 4.2 V at room temperature (25 °C) to verify cell operation. Voltage and current were monitored with time, and the resulting behavior for room temperature testing is shown in **Figure 4**a. Coin cells containing anodes coated with PE microspheres were then heated to 110 °C by immersion in heated silicone oil (1 L) during cell cycling. Cell shutdown was verified (Figure 4b) in contrast to control cells in which no functionalization of the anode was used (Figure 4e). Cells were then heated to 135 °C (activation temperature of the Celgard 2325 commercial shutdown separator) with no further change in the voltage or current profile of the cell, indicating that the cell was permanently shut down due to microsphere activation (Figure 4c). Coin cells containing PE microspheres showed similar voltage and current profiles to that of control cells both when cycled at room temperature and post-shutdown. Post-cycling dismantling of the control cells revealed that the separator was deformed as a result of shutdown activation, risking a short circuit (SI Figure S4).

The specific charge capacity for coin cells with increasing levels of PE microsphere on the anode is shown in **Figure 5**a. At low PE microsphere coverages (ρ = 2.0 mg cm^{-2}), specific

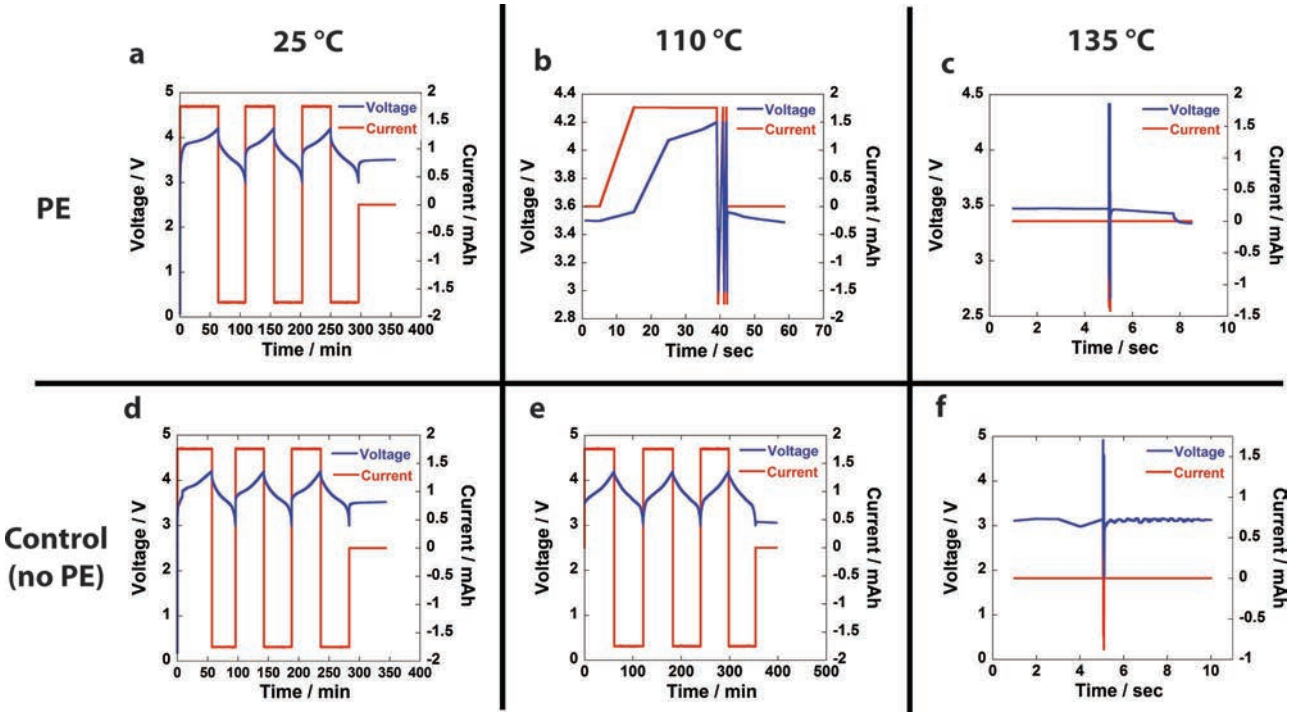

Figure 4. Voltage and current profiles for coin cells containing a PE microsphere functionalized anode (a–c) and an uncoated anode (control cell) (d–f). a) Room temperature cycling profile for a cell containing a commercial separator and PE microspheres (12.7 mg cm^{-1} coverage) on the anode. b) Cycling profile demonstrating shutdown achieved using PE microspheres on the anode at 110 °C. c) Cycling profile at 135 °C for cell previously shutdown at 110 °C. d) Room temperature cycling profile of a control cell containing only a commercial shutdown separator as a shutdown mechanism (no PE microspheres). e) Cycling profile of a control cell at 110 °C. f) Cycling profile of a control cell previously exposed to 110 °C with shutdown achieved by a commercial tri-layer separator at 135 °C.

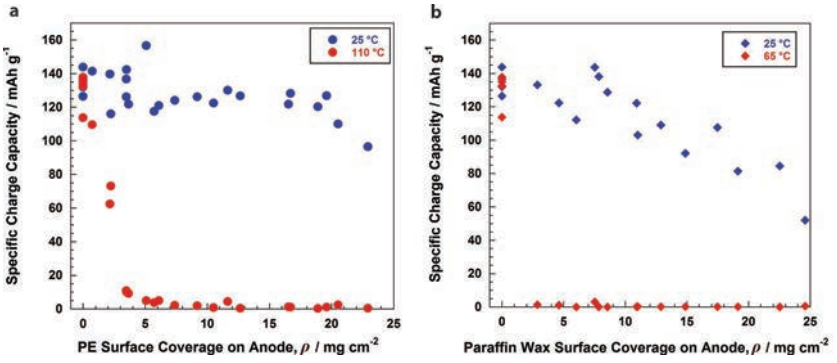

Figure 5. Specific charge capacity of cells containing microsphere coated anodes at room temperature and 110 °C. a) Specific charge capacity of cells containing PE microsphere coated anodes. b) Specific charge capacity of cells containing paraffin wax microsphere coated anodes.

charge capacity is reduced as a result of thermal treatment (110 °C), but some capacity remains. At ρ = 3.5 mg cm^{-2} the specific charge capacity is reduced by 92% at 110 °C. The minimum observed coverage required for full cell shutdown (>98% loss in initial capacity) is 7.4 mg cm^{-2}. In this case, shutdown occurs within approximately 6 min. The time scale in which thermal runaway occurs as a result of a short circuit is approximately 1 min.[9] Coverage of 9.2, 10.5, and 20.5 mg cm^{-2} induce shutdown within 2.5 min, 65 s, and 37 s, respectively (see SI, Table S1). Although fast shutdown times (<1 min) can be achieved with higher surface coverage of PE microspheres, other polymers are being investigated to meet this requirement at a lower surface coverage. At room temperature, capacity of coin cells is unaffected until ρ = 12 mg cm^{-2}, when cycling at a rate of 1C.

To demonstrate that the microsphere-based autonomic shutdown concept is not limited to PE microspheres alone, paraffin wax microspheres (m.p. 60 °C) were incorporated into Li-ion coin cell batteries and tested both at room temperature and at 65 °C. Specific charge capacity as a function of paraffin wax microsphere coverage is shown in Figure 5b. Like cells containing PE-coated anodes, cell shutdown is achieved above a certain critical coverage (ρ = 2.9 mg cm^{-2}). Shutdown using paraffin wax microspheres is achieved rapidly, with coverages of 7.5, 8.6, and 21.0 mg cm^{-2} resulting in shutdown in 244, 22, and 5.2 seconds respectively (SI, Table S2). Room temperature capacity of coin cells is unaffected until ρ = 7.6 mg cm^{-2} when cycling at 1C.

We also coated commercial Celgard 2325 separators with PE microspheres and demonstrated autonomic shutdown at 110 °C. Specific charge capacity as a function of capsule coverage is

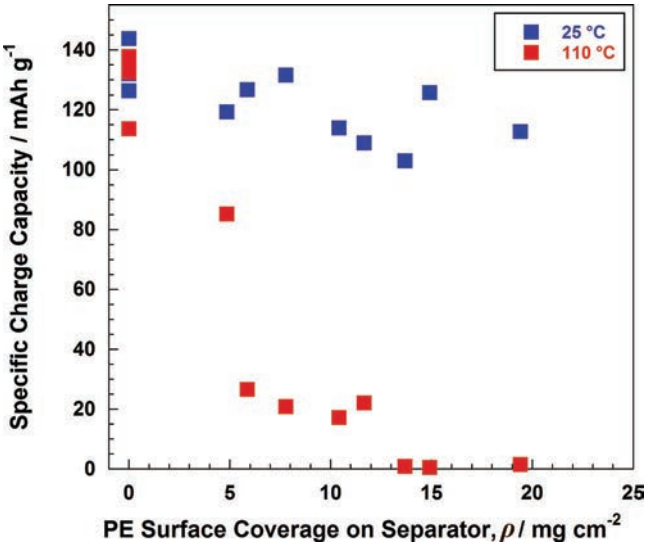

Figure 6. Specific charge capacity of cells containing PE microsphere coated separators at room temperature and at 110 °C.

shown in **Figure 6**. The critical coverage for full shutdown with PE-functionalized separators was found to be $\rho = 13.7$ mg cm^{-2}, a value higher than for PE or paraffin-functionalized anodes.

2.4. Impedance Testing

To verify cell shutdown, impedance tests were performed on coin cells at various (low, medium, and high) coverages. Cell impedance increased by several orders of magnitude as a result of polymer film formation during shutdown (**Table 1**). For example, at ca. 9 mg cm^{-2} coverage, the cell impedance increases by roughly two orders of magnitude from 25 °C to 110 °C. We also see a significant increase in post-shutdown impedance for cells above the critical coverage concentration ($\rho = 2.9$ mg cm^{-2}) in comparison to control cells ($\rho = 0$ mg cm^{-2}).

Impedance data for coin cells cycled at room temperature reveals that a significant increase occurs for the two highest coverages tested. Nevertheless, at a 1C cycling rate, the effect of increased impedance on battery capacity does not appear to be evident. With the current system, testing at higher cycling rates may show a sacrifice in battery capacity. However, future studies will focus on improving this performance via optimization of sphere size, surface functionalization, binder concentration, and surface coverage.

Table 1. Impedance data (at 1 kHz) for coin cells cycled at 25 °C and 110 °C.

Coverage, ρ [mg cm^{-2}]	Impedance [Ω] (1 kHz)	
	@ 25 °C	@ 110 °C
None (0)	8.14	368
Low (1.8–2.2)	8.88	342
Medium (8.9–9.2)	9.75	1010
High (16.7–18.1)	18.8	10 500

2.5. Thermal Stability

To maintain cycle life and ensure safe operation, Li-ion batteries typically operate below 45 °C.[54,55] The stability of the PE microsphere functionalized anodes was investigated at 45 °C, and compared to cell performance at room temperature (25 °C). A coin cell with $\rho = 6.6$ mg cm^{-2} was cycled at 25 °C and 45 °C. Specific charge capacities (averaged over 3 cycles) are 122 mAh g^{-1} and 120 mAh g^{-1}, respectively, indicating no significant loss in capacity as a result of elevated temperature.

2.6. Post-Shutdown Electrode Surface Morphology

Post-shutdown, both control cells and cells containing PE microspheres were disassembled and the anode and separator were isolated from the battery casing and allowed to dry. A representative control anode and coated anode before and after shutdown were examined by SEM. An anode from a control cell that was cycled at 110 °C is shown in **Figure 7**a,d. An anode coated with PE microspheres ($\rho = 7.7$ mg cm^{-2}) is shown in Figure 7b,e. The microspheres appear uniformly distributed in a layer approximately 75 µm in height. Although this layer is roughly three times thicker than a commercial trilayer separator, the cell performs comparably to a control cell at 1C. However, coating thicknesses may have to be decreased to avoid sacrificing high energy density and for high rate performance (above 1C). For cells where full shutdown occurs at 110 °C, the PE microspheres have melted completely and infiltrated the anode, effectively blocking Li-ion transport (Figure 7c,f).

For cells where full shutdown does not occur, the melted PE microspheres only partially infiltrate the anode, leaving some ion-conductivity remaining (see **Figure 8**a). For cells with high PE microsphere coverages ($\rho = 20$ mg cm^{-2}), an excess of molten PE exists which forms a dense film ca. 20 µm thick on the surface of the anode (see Figure 8b). In this case, some transfer of molten PE occurs onto the separator as well (see SI Figure S5b,d). However, the film on the separator is thin (ca. 4 µm) compared to the anode.

3. Conclusion

Autonomic shutdown of a Li-ion battery was demonstrated using polymer microspheres that melt upon heating and form a barrier to Li-ion conduction. Both PE (ca. 4 µm) and paraffin microspheres (ca. 42 µm) spin-coated onto graphite anodes at concentrations of 7.4 mg cm^{-2} (PE) and 2.9 mg cm^{-2} (paraffin) reduced specific charge capacity in Li-ion coin cell batteries by more than 98% when heated to 110 °C (PE) or 65 °C (paraffin). PE microspheres coated onto a commercial trilayer separator at a concentration of 13.7 mg cm^{-2} also demonstrated autonomic shutdown at 110 °C. Electron microscopy of anodes after shutdown revealed evidence of in situ formation of a conformal PE film and PE infiltration of the anode surface. Since the melt

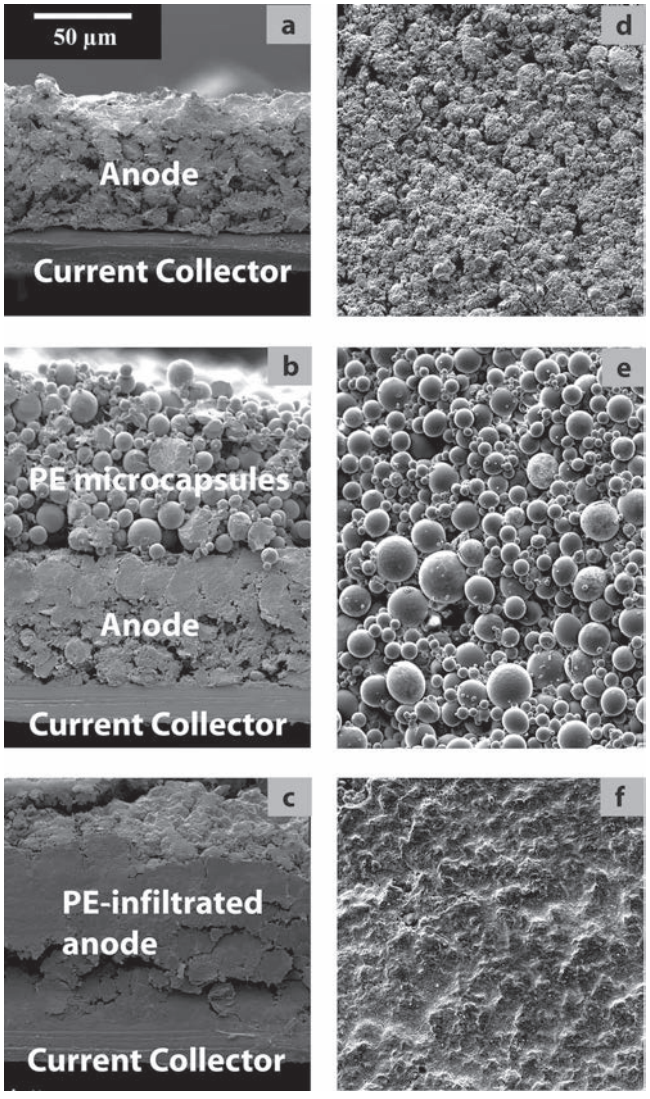

Figure 7. Scanning electron microscopy images of anode cross sections and surfaces. a) Cross-sectional view of an anode cycled at 110 °C (control), b) anode with ρ = 7.7 mg cm^{-2} before incorporation into c) a coin cell anode with ρ = 7.7 mg cm^{-2} and cycled at 110 °C. d) Top view of a cycled and heated (110 °C) anode (control). e) Top view of anode with ρ = 7.7 mg cm^{-2} before incorporation into a coin cell. f) Cycled, heated (110 °C) anode with ρ = 7.7 mg cm^{-2}. The electrode increases in thickness by ~20 µm.

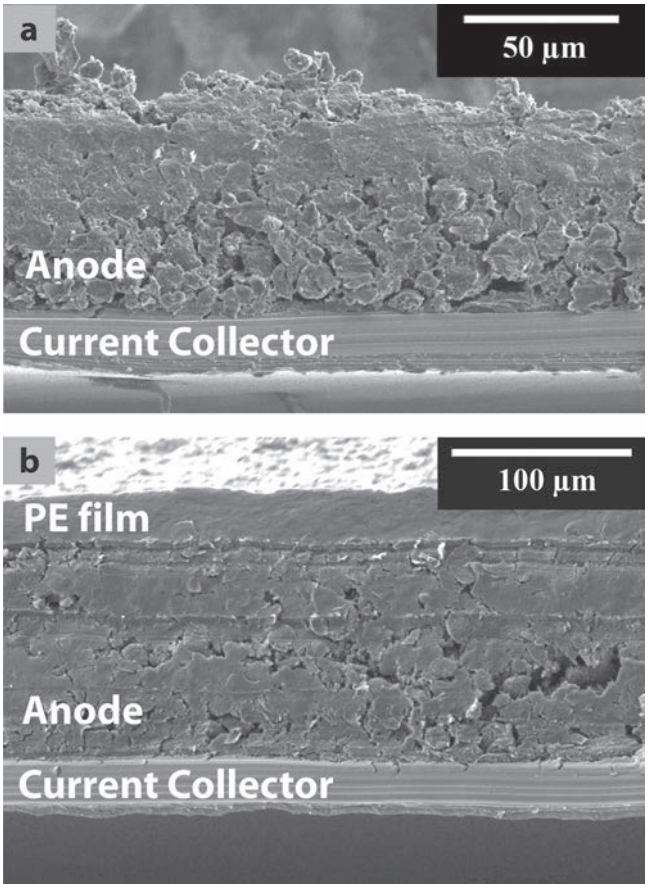

Figure 8. Scanning electron microscopy images of anode cross sections. a) Cycled anode cross section after shutdown at 110 °C (ρ = 2.2 mg cm^{-2}). b) Cycled anode cross section after shutdown at 110 °C (ρ = 20.5 mg cm^{-2})

transition temperature of the encapsulated polymer dictates the triggering temperature of cell shutdown, this highly customizable mechanism should be applicable to a wide variety of battery chemistries and their unique shutdown requirements.

4. Experimental Section

Materials and Equipment: Low-density poly(ethylene) (LDPE, M_w = 4000, m.p. 110 °C), Brij 76 surfactant, and sodium dodecyl sulfate (SDS), paraffin wax (m.p. 58–60 °C), and n-methylpyrrolidone (NMP) solvent were purchased from Sigma-Aldrich. Xylene was purchased from Fisher Scientific. Poly(vinylidene fluoride) (PVDF) binder was purchased from Alfa Aesar. Bulk mesocarbon microbead (MCMB) anode material (Enerland), $Li(Ni_{1/3}Co_{1/3}Mn_{1/3})O_2$ (Li333) cathode material (Enerland), Celgard 2325 separator material, and 1.2 M $LiPF_6$ in EC:EMC electrolyte were obtained from Argonne National Laboratory. Anodes were cut to the appropriate size using a 1.27 cm punch purchased from McMaster-Carr. Coated anodes were prepared using a Specialty Coating Systems spin-coater. C2032-type coin cell hardware components and the coin cell crimper were purchased from MTI Corporation, with the exception of coin cell springs, which were purchased from Hohsen/Pred Materials Corp. The thermal testing apparatus includes 50 cP silicone oil (Sigma-Aldrich), hose clamps, and electrical leads. All coin cells were cycled using an Arbin BT2000 cycler.

Anode and Separator Coating Methods: Microsphere coated anodes and separators were prepared by spin-coating a microsphere suspension directly onto the graphitic anode substrate or polymer separator. The materials required for preparation of the anodes and separators include the suspension to be spin-coated, Beckton-Dickinson syringes, 18 gauge needles, and a spin-coater apparatus. Using a 1 mL syringe outfitted with an 18 gauge needle, the suspension (0.075 mL) was deposited onto a spinning anode or separator disk. Once coated, anodes and separators were removed from the spin-coater stage and air-dried for a minimum of 24 h before incorporation into coin cells. Surface coverage was determined gravimetrically by weighing each dried anode and dividing by the anode disk surface area.

Cell Assembly and Testing Method: Coated anodes (or separators) were assembled into coin cells in an argon-filled glove box. The stacking

sequence of the coin cell consisted of the anode cap, spring, spacer, anode disk, Celgard 2325 separator, 1.2 M $LiPF_6$ in EC: EMC electrolyte (120 µL), cathode disk, spacer, and top cap.

After assembly, cells were removed from the glove box and mounted in the cycler for testing. Cells were charged and discharged 3 times at a constant current of ±1.75 mA. For thermal testing, the cycling program commenced as soon as the cell was fully submerged in oil. The cell was allowed to cycle until it completes 3 full cycles. Voltage after the third cycle is briefly monitored to confirm that the cell did not short circuit, but rather shut down. The cell is then removed from the oil, allowed to cool, and removed from the thermal testing clamp.

Impedance Testing Method: Coins cells were assembled with various coverages of PE microspheres and tested as described above prior to impedance testing. Impedance testing was performed in a frequency range of 0.05 Hz to 100 kHz using both a CH Instruments Model 660 Electrochemical Workstation and a Schlumberger SI 1260 Impedance/Gain-Phase analyzer.

Profilometry Testing Method: Profilometry testing was performed on sample uncoated and spin-coated graphite electrodes (dia. 1.27 cm) using a Sloan Dentak^3 surface profilometer. Measurements were taken at a stylus speed of 2.5 µm s^{-1} and over a distance of 4000 µm.

Supporting Information

Supporting Information is available from the Wiley Online Library or from the author.

Acknowledgements

This research was supported as part of the Center for Electrical Energy Storage, an Energy Frontier Research Center funded by the US Department of Energy, Office of Science, Office of Basic Energy Sciences. M. Baginska would also like to acknowledge the American Association of University Women (AAUW) for its Selected Professions fellowship and the University of Illinois Urbana-Champaign College of Engineering for its SURGE fellowship. The authors would like to acknowledge helpful discussions with Dr. Zheng Xue, Dr. Susan A. Odom, Brandon Long, Steven Zhang, Sen Kang, Elizabeth Jones, and Meg Grady at the University of Illinois Urbana-Champaign, and Dr. Chris Johnson, Dr. Lynn Trahey, Dr. Wei Weng, Dr. Ali Abouimrane, Dr. Khalil Amine, and Dr. Mike Thackeray at Argonne National Laboratory.

Received: November 14, 2011
Published online: March 14, 2012

[1] M. Armand, J.-M. Tarascon, *Nature* **2008**, *451*, 652.
[2] G. X. Wang, J.-H. Ahn, M. J. Lindsay, L. Sun, D. H. Bradhurst, S. X. Dou, H. K. Liu, *J. Power Sources* **2001**, *97–98*, 211.
[3] W. H. Meyer, *Adv. Mater.* **1998**, *10*, 439.
[4] S. A. Khateeb, M. M. Farid, J. R. Selman, S. Al-Hallaj, *J. Power Sources* **2004**, *128*, 292.
[5] T. M. Bandhauer, S. Garimella, T. F. Fuller, *J. Electrochem. Soc.* **2011**, *158*, R1.
[6] D. P. Abraham, E. P. Roth, R. Kostecki, K. McCarthy, S. MacLaren, D. H. Doughty, *J. Power Sources* **2006**, *161*, 648.
[7] R. A. Leising, M. J. Palazzo, E. S. Takeuchi, K. J. Takeuchi, *J. Electrochem. Soc.* **2001**, *148*, A838.
[8] Federal Aviation Administration, http://www.faa.gov/about/office_org/headquarters_offices/ash/ash_programs/hazmat/air-carrier_info/media/Battery_incident_chart.pdf, in Batteries and Battery-Powered Devices: Aviation Accidents Involving Fire, Smoke, Heat, or Explosion **2010**, accessed April 2011.
[9] Y. Chen, L. Song, J. W. Evans, in *Proc. 31st Intersoc. Energy Conv. Engin. Conf.*, Vol. *2*, IEEE, New York, NY **1996**, p. 1465.
[10] C.-H. Doh, D.-H. Kim, H.-S. Kim, H.-M. Shin, Y.-D. Jeong, S.-I. Moon, B.-S. Jin, S. W. Eom, H.-S. Kim, K.-W. Kim, D.-H. Oh, A. Veluchamy, *J. Power Sources* **2008**, *175*, 881.
[11] F. Joho, P. Novak, M. E. Spahr, *J. Electrochem. Soc.* **2002**, *149*, A1020.
[12] B. K. Mandal, A. K. Padhi, Z. Shi, S. Chakraborty, R. Filler, *J. Power Sources* **2006**, *161*, 1341.
[13] J. P. Christophersen, C. G. Motloch, C. D. Ho, D. F. Glenn, R. B. Wright, J. R. Belt, T. C. Murphy, T. Q. Duong, V. S. Battaglia, http://avt.inl.gov/battery/pdf/atd_gen2_interim_report_rev2.pdf, in DOE Advanced Technology Development Program for Lithium-Ion Batteries: INEEL Interim Report for Gen 2 Cycle-Life Testing **2002**, accessed April 2011.
[14] P. G. Balakrishnan, R. Ramesh, T. Prem Kumar, *J. Power Sources* **2006**, *155*, 401.
[15] Q. Wang, J. Sun, C. Chen, *J. Electrochem. Soc.* **2007**, *154*, A263.
[16] I. Uchida, H. Ishikawa, M. Mohamedi, M. Umeda, *J. Power Sources* **2003**, *119–121*, 821.
[17] P. Arora, Z. Zhang, *Chem. Rev.* **2004**, *104*, 4419.
[18] X. Huang, *J. Solid State Electrochem.* **2010**, *15*, 649.
[19] S. S. Zhang, *J. Power Sources* **2007**, *164*, 351.
[20] Y. S. Chung, S. H. Yoo, C. K. Kim, *Industrial Engin. Chem. Res.* **2009**, *48*, 4346.
[21] E. P. Roth, D. H. Doughty, D. L. Pile, *J. Power Sources* **2007**, *174*, 579.
[22] M. A. Faust, M. R. Suchanski, H. W. Osterhoudt, Eastman Kodak Company, USA 4741979, **1987**.
[23] M. Ullrich, T. Brohm, H. Rabenstein, D. Bechtold, NBT GmbH, USA 6511517, **2000**.
[24] J. K. Feng, Y. L. Cao, X. P. Ai, H. X. Yang, *Electrochim. Acta* **2008**, *53*, 8265.
[25] Y. Zhang, A.-Q. Zhang, Y.-H. Gui, L.-Z. Wang, X.-B. Wu, C.-F. Zhang, P. Zhang, *J. Power Sources* **2008**, *185*, 492.
[26] Y. Ma, G. Yin, P. Zuo, X. Tan, Y. Gao, P. Shi, *Electrochem. Solid-State Lett.* **2008**, *11*, 129.
[27] Z. Chen, K. Amine, *Electrochem. Commun.* **2007**, *9*, 703.
[28] J. Nguyen, C. Taylor, INTELEC 26th Annual International Telecommunications Energy Conference, Piscataway, NJ, **2004**, p.146.
[29] Y. Gao, M. V. Yakovleva, W. B. Ebner, *Electrochem. Solid-State Lett.* **1998**, *1*, 117.
[30] H. Lee, M. G. Kim, J. Cho, *Electrochem. Commun.* **2007**, *9*, 149.
[31] L. J. Fu, H. Liu, C. Li, Y. P. Wu, E. Rahm, R. Holze, H. Q. Wu, *Solid State Sci.* **2006**, *8*, 113.
[32] T. Sato, K. Banno, T. Maruo, R. Nozu, *J. Power Sources* **2005**, *152*, 264.
[33] C. L. Cheng, C. C. Wan, Y. Y. Wang, M. S. Wu, *J. Power Sources* **2005**, *144*, 238.
[34] S. R. White, N. R. Sottos, P. H. Geubelle, J. S. Moore, M. R. Kessler, S. R. Sriram, E. N. Brown, S. Viswanathan, *Nature* **2001**, *409*, 794.
[35] M. A. White, *J. Chem. Education* **1998**, *75*, 1119.
[36] S. N. Rodrigues, I. M. Martins, I. P. Fernandes, P. B. Gomes, V. G. Mata, M. F. Barreiro, A. E. Rodrigues, *Chem. Engin. J.* **2009**, *149*, 463.
[37] E. T. A. van den Dungen, B. Loos, B. Klumperman, *Macromol. Rapid Commun.* **2010**, *31*, 625.
[38] R. S. Jadhav, D. G. Hundiwale, P. P. Mahulikar, *J. Appl. Polym. Sci.* **2011**, *119*, 2911.
[39] A. P. Esser-Kahn, N. R. Sottos, S. R. White, J. S. Moore, *J. Am. Chem. Soc.* **2010**, *132*, 10266.
[40] W. Qi, X. Yan, J. Fei, A. Wang, Y. Cui, J. Li, *Biomaterials* **2009**, *30*, 2799.
[41] J. Wei, X.-J. Ju, R. Xie, C.-L. Mou, X. Lin, L.-Y. Chu, *J. Colloid Interface Sci.* **2011**, *357*, 101.

[42] M. Yoshida, T. Matsui, Y. Hatate, T. Takei, K. Shiomori, S. Kiyoyama, *J. Polymer Sci. A: Polym. Chem.* **2008**, *46*, 1749.
[43] J. Yun, J. S. Im, Y.-S. Lee, T.-S. Bae, Y.-M. Lim, H.-I. Kim, *Colloids Surfaces A* **2010**, *368*, 23.
[44] P. Degen, Z. Chen, H. Rehage, *Macromol. Chem. Phys.* **2010**, *211*, 434.
[45] H. Guo, X. Zhao, J. Wang, *J. Colloid Interface Sci.* **2005**, *284*, 646.
[46] S.-H. Hu, C.-H. Tsai, C.-F. Liao, D.-M. Liu, S.-Y. Chen, *Langmuir* **2008**, *24*, 11811.
[47] P. Degen, S. Peschel, H. Rehage, *Colloid Polymer Science* **2008**, *286*, 865.
[48] N. Gaponik, I. L. Radtchenko, G. B. Sukhorukov, A. L. Rogach, *Langmuir* **2004**, *20*, 1449.
[49] C. Tu, J. Du, L. Yao, C. Yang, M. Ge, C. Xu, M. Gao, *J. Mater. Chem.* **2009**, *19*, 1245.
[50] L.-Y. Chu, S.-H. Park, T. Yamaguchi, S.-I. Nakao, *Langmuir* **2002**, *18*, 1856.
[51] Q. Gao, C. Wang, H. Liu, C. Wang, X. Liu, Z. Tong, *Polymer* **2009**, *50*, 2587.
[52] M. K. Kang, J.-C. Kim, *J. Appl. Polym. Sci.* **2010**, *118*, 421.
[53] C.-J. Huang, F.-C. Chang, *Macromolecules* **2009**, *42*, 5155.
[54] http://www.panasonic.com/industrial/includes/pdf/Panasonic_LiIon_Precautions.pdf, in *Lithium-Ion Batteries Technical Handbook*, Panasonic, **2007**, accessed April 2011.
[55] P. G. Patril, www.ipd.anl.gov/anlpubs/2008/02/60978.pdf, in Developments in Lithium-Ion Battery Technology in The Peoples Republic of China, Argonne National Laboratory, **2008**, accessed January 2011.